Journal of Photonics for Energy

SPIEDigitalLibrary.org/jpe

Microphotoluminescence study of Cu_2ZnSnS_4 polycrystals

Maarja Grossberg
Pille Salu
Jaan Raudoja
Jüri Krustok

SPIE

Microphotoluminescence study of Cu_2ZnSnS_4 polycrystals

Maarja Grossberg, Pille Salu, Jaan Raudoja, and Jüri Krustok
Tallinn University of Technology, Department of Materials Science,
Ehitajate tee 5, 19086 Tallinn, Estonia
maarja.grossberg@ttu.ee

Abstract. Microphotoluminescence studies of Cu_2ZnSnS_4 polycrystals were performed. At room temperature, two photoluminescence (PL) bands were detected at 1.39 and 1.53 eV and attributed to band-to-tail (BT) and band-to-band (BB) recombination, respectively. At lower temperatures, band-to-impurity recombination always dominates. The results show that the model of heavily doped semiconductors applies to Cu_2ZnSnS_4 and that, in contrast to the ternary chalcopyrites, the BT recombination in Cu_2ZnSnS_4 has very low intensity. The laser power dependency of the PL intensity shows that the recombination mechanism of BT and BB bands exhibits an exciton-like behavior. © *2013 Society of Photo-Optical Instrumentation Engineers (SPIE)* [DOI: 10.1117/1.JPE.3.030599]

Keywords: Cu_2ZnSnS^4; kesterites; potential fluctuations; photoluminescence.

Paper 13009L received Apr. 22, 2013; revised manuscript received May 13, 2013; accepted for publication May 14, 2013; published online Jun. 3, 2013.

1 Introduction

Cu_2ZnSnS_4 (CZTS) is considered a promising absorber material for thin-film solar cells, which has optimal direct bandgap energy (~1.5 eV) for solar energy absorption and high absorption coefficient ($>10^4$ cm^{-1}).[1] Compared to the current high-efficiency thin-film solar cell absorber materials $CuIn_{1-x}Ga_xSe_2$ (CIGS) and CdTe, the kesterite compound CZTS is composed of low-cost, Earth-abundant, and nontoxic elements. The current record of the solar energy conversion efficiency of CZTS-based solar cells is 8.4%.[2] The overall highest solar energy conversion efficiency of 43.5% was obtained by using III-V multijunction tandem cell approach based on GaInNAs and GaAs.[3] However, alternative low-cost materials and technologies are under intense investigation, CZTS being one of the promising absorber materials. One prerequisite for obtaining high-efficiency solar cells is the control over the defect structure of the absorber material, including electrically active point defects and the presence of secondary phases.

Photoluminescence (PL) spectroscopy is proven to be a very sensitive tool for studying point defects in semiconductors. In low-temperature PL studies of CZTS, a broad and asymmetric PL band at around 1.3 eV has been detected in many studies.[4–10] In our recent paper,[11] it was observed that the PL emission at 1.3 eV in CZTS polycrystals consists of two PL bands at 1.27 and 1.35 eV, which both result from band-to-impurity (BI) recombination involving a deep acceptor defect with the ionization energy of around 280 meV but different CZTS phase (kesterite and disordered kesterite). The PL band at around 1.3 eV has also been attributed to donor–acceptor pair recombination[5,6] and free-to-bound recombination[7,8] involving defects with very different ionization energies. Therefore, there is contradictory data available concerning this PL band. However, the asymmetric shape and the large blue shift (>15 meV/decade) with increasing laser power of the PL band at around 1.3 eV indicate the presence of spatial electrostatic potential fluctuations in the material that are believed to have a detrimental effect on the device performance. The recombination processes in the presence of spatial potential fluctuations are described by the theory of heavily doped semiconductors.[12,13] The condition

0091-3286/2013/$25.00 © 2013 SPIE

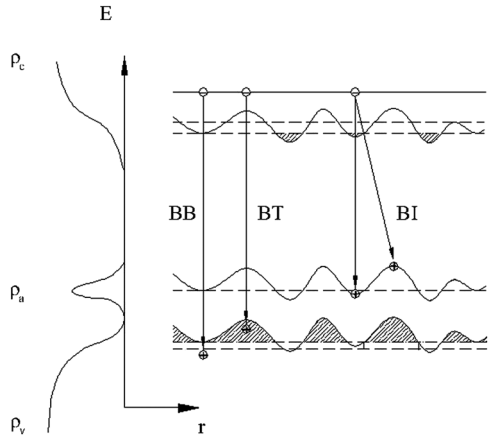

Fig. 1 Schematic picture of the band diagram of heavily doped semiconductors. Because of heavy doping, the band edges start to fluctuate in space. The BI, BT, and BB recombination paths are indicated with arrows. On the left, the density of state functions ρ_c, ρ_a, and ρ_v of the conduction band, defect state, and valence band, respectively, are presented.

of heavy doping in this case results from a large concentration of native defects in the material. High concentration of randomly distributed charged defects leads to the formation of spatial electrostatic potential fluctuations. As a result, tails of the density of state functions of the valence and conduction bands are formed (see Fig. 1). According to the theory, the luminescence spectrum of heavily doped semiconductors is usually dominated by three recombination channels (see Fig. 1). The first is a band-to-band (BB) recombination, where a free electron recombines with a free hole. This recombination is usually seen only at higher temperatures. The second is a band-to-tail (BT) recombination, where a free electron recombines with a hole that is localised in the valence band tail. The third is BI recombination, where a free electron recombines with a hole that is localized on a deep acceptor state. These recombination mechanisms are often observed in ternary chalcopyrite semiconductors, where the condition of heavy doping by native defects is usually fulfilled.[14–17] The kesterites like CZTS are considered to be quaternary analogues to the ternary chalcopyrites; however, interestingly, BT and BB emissions in kesterites have not been detected so far. In CZTS, only Romero et al.[18] claim that they have observed BT and BB recombination at 1.25 and 1.33 eV, respectively. However, these PL bands are few hundred meV below the estimated bandgap energy of ~1.55 eV (Ref. 19), which is in contradiction to the theory. In this paper, we present the micro-PL results of CZTS polycrystals measured at high excitation level.

2 Experimental Details

Cu_2ZnSnS_4 polycrystalline powder was synthesized from the metallic precursor powders with the purity of 99.9%. The metal powders and sulfur were mixed properly in mortar. Then the powder was inserted into quartz ampoule that was degassed and sealed. The ampoule with the material was kept at 750°C for 50 h and then quenched into water. For thermal post-treatment, the ampoule with the material was heated up to 550°C and kept for 170 h at this temperature and then cooled slowly with the furnace during 40 h to 100°C. The single phase composition of CZTS polycrystals is determined by Raman scattering analysis (spectrum presented in Ref. 11). From the Raman spectra of the studied CZTS polycrystals, traces of disordered kesterite phase were found in addition to the kesterite CZTS. The room-temperature micro-PL spectra were recorded by using a Horiba's LabRam HR spectrometer equipped with a multichannel charge coupled device detection system in the backscattering configuration and an Olympus microscope. For PL excitation, the 532-nm laser line that was focused on the sample with the spot diameter of 10 μm was used. For the laser power dependence measurements, neutral density filters were used.

3 Results and Discussion

The micro-PL spectra of various CZTS polycrystals from the same synthesis are shown in Fig. 2. The room-temperature spectra [Fig. 2(a) and 2(b)] consist of two PL bands with slightly varying peak positions when measuring from different crystals. The PL band at around 1.53 eV is attributed to BB recombination and the PL band at around 1.39 eV to BT recombination based on the analysis below. The energetic difference between BT and BB bands is about 140 meV, which is close to the one observed in CIGS and other chalcopyrite ternaries.[14,16] The micro-PL spectrum at $T = 200$ K [Fig. 2(c)] is dominated by BI recombination together with the BT recombination. In our recent paper,[11] where the low temperature PL ($T = 10$ K) of CZTS polycrystals was studied, two BI bands with similar behaviors in laser power and temperature were observed and the coexistence of kesterite and disordered kesterite phase in these polycrystals was established. The same should be considered when analyzing the room-temperature micro-PL spectra of these polycrystals. The PL emissions related to the two observed phases of CZTS are not resolved at room temperature; however, the coexistence of the kesterite and disordered kesterite phase influences the peak positions and halfwidths of the BB and BT bands. According to the calculations by Chen et al.,[20] the bandgap energy difference of the kesterite and stannite phase in CZTS is 0.12 eV, the latter being smaller. The energy difference of the BI bands at $T = 10$ K was 0.08 eV (Ref. 11) and they were therefore attributed to kesterite and disordered kesterite phase. If the PL emission related to the kesterite phase prevails, the BB and BT bands are shifted toward higher energies. The peak positions of BB and BT bands vary from 1.513 to 1.557 eV and from 1.378 to 1.418 eV, respectively, the shift in the PL band position being about 40 meV for both PL bands.

The laser power dependencies of the PL spectra at room temperature show that at low excitation intensity, the BT band prevails and with increasing excitation intensity, the relative intensity of the BB band increases (see Fig. 3). From the fittings of the spectra with empirical asymmetric double sigmoidal function (see details in Ref. 14), no shift of the PL bands with laser power could be detected up to the laser power density of 300 W/cm^2. This is in accordance with the theory,[12,13] since at room temperature there is no redistribution of holes between the potential wells of the fluctuating potentials. However, when the heating of the sample by the laser starts at power densities over 300 W/cm^2, a blue shift of the PL bands, mainly

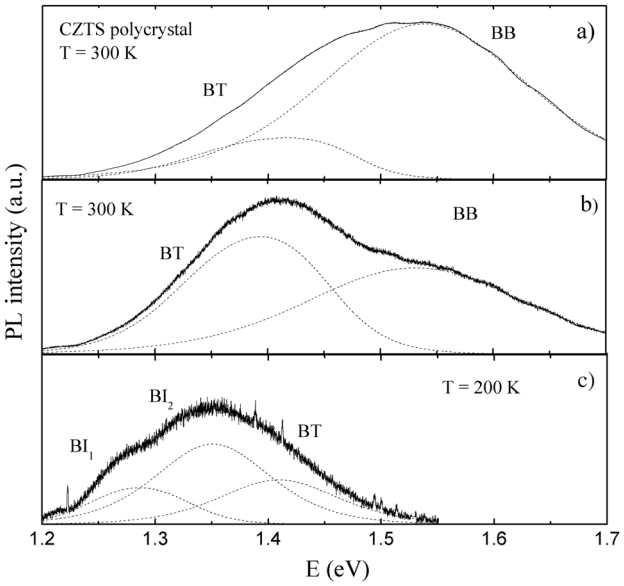

Fig. 2 Micro-PL spectra (a) and (b) of two CZTS polycrystals at room temperature and (c) of (b) at $T = 200$ K. At low temperatures, BI recombination dominates (BI_1 and BI_2 arise from the disordered kesterite and kesterite phase, respectively); at higher temperatures, first BT and then BB band appear.

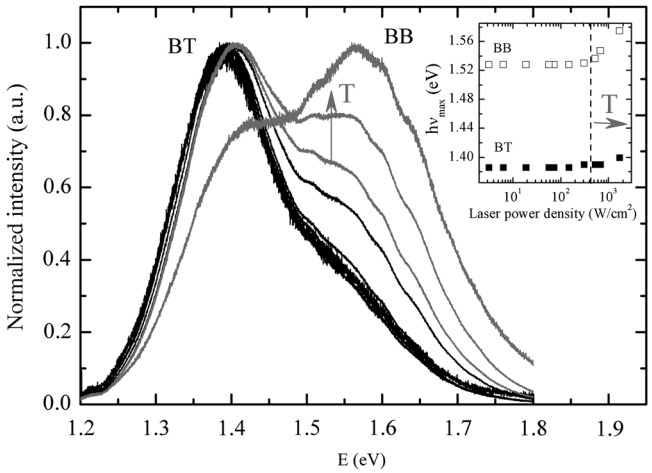

Fig. 3 Laser power dependence of the micro-PL spectra of a CZTS polycrystal at room temperature. The inset graph shows the laser power dependence of the peak positions of the PL bands obtained from the fittings of the spectra. The spectra in gray color are influenced by the rise of the sample temperature due to high excitation power density. In the inset graph, the corresponding points are separated with dashed vertical line.

caused by the Moss–Burstein effect, is detected. On the other hand, the PL intensity, I_{PL}, increases with increasing excitation power, L, and the relation can be expressed as $I_{PL} \sim L^k$, with $k = 1.60$ and 1.65 for BT and BB bands, respectively (see Fig. 4). For excitation laser emission with energy exceeding the band gap energy, the exponent k is generally between 1 and 2 for the free- and bound-exciton emission, and k is less than 1 for free-to-bound and donor–acceptor pair recombinations.[21] This indicates that the observed BB and BT emissions can be categorized as exciton-like transitions that do not involve carriers localized on energy levels in the bandgap. However, in the case of measurements at high excitation level, with the laser power density being over 300 W/cm^2, the sample is heated up and a rise in the sample temperature has to be taken into account. In Fig. 4 and in the inset of Fig. 3, the three points corresponding to the highest excitation power density show the influence of the increasing sample temperature. With increasing sample temperature, the overall PL intensity decreases and the relative intensity of the BB increases since the holes are thermally released from the potential wells in the valence band tail.

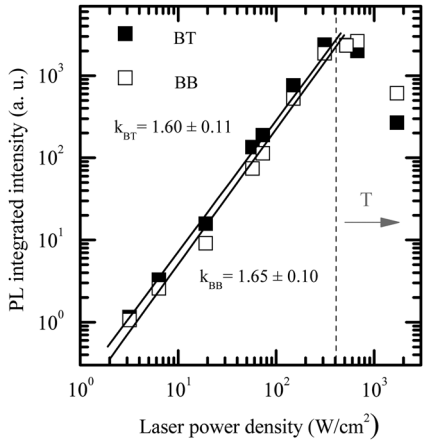

Fig. 4 Excitation power dependence of the integrated intensity of the BB and BT bands. The three points corresponding to higher excitation power density show the rise in the sample temperature.

4 Conclusions

In conclusion, BB and BT bands were detected in the room-temperature micro-PL spectra of CZTS polycrystals at 1.39 and 1.53 eV. These results show that the model of heavily doped semiconductors applies to CZTS and that, in contrast to the ternary chalcopyrites, BT recombination becomes visible only at high temperatures and at high excitation level.

Acknowledgments

This work was supported by the Estonian Science Foundation grants G-8282 and ETF 9369, the target financing by Estonian Ministry of Education and Research (HTM) (Estonia) No. SF0140099s08, the Estonian Centre of Excellence in Research, Project TK117, and the Estonian National Energy Technology Programme, Project AR10128.

References

1. K. Ito and T. Nakazawa, "Electrical and optical properties of stannite-type quaternary semiconductor thin films," *Jpn. J. Appl. Phys.* **27**(11), 2094–2097 (1988), http://dx.doi.org/10.1143/JJAP.27.2094.
2. B. Shin et al., "Thin film solar cell with 8.4% power conversion efficiency using an earth-abundant Cu_2ZnSnS_4 absorber," *Prog. Photovolt: Res. Appl.* **21**(1), 72–76 (2013), http://dx.doi.org/10.1002/pip.v21.1.
3. M. Wiemer, Sabnis V., and Yuen H., "43.5% efficient lattice matched solar cells," *Proc. SPIE* **8108**, 810804 (2011), http://dx.doi.org/10.1117/12.897769.
4. K. Hönes et al., "Shallow defects in Cu_2ZnSnS_4," *Physica B: Condensed Matter* **404**(23–24), 4949–4952 (2009), http://dx.doi.org/10.1016/j.physb.2009.08.206.
5. K. Tanaka et al., "Donor-acceptor pair recombination luminescence from Cu_2ZnSnS_4 bulk single crystals," *phys. stat. sol. (a)* **203**(11), 2891–2896 (2006), http://dx.doi.org/10.1002/pssa.v203:11.
6. Y. Miyamoto et al., "Optical properties of Cu_2ZnSnS_4 thin films prepared by sol–gel and sulfurization method," *Jpn. J. Appl. Phys.* **47**(1), 596–597 (2008), http://dx.doi.org/10.1143/JJAP.47.596.
7. J. P. Leitao et al., "Photoluminescence and electrical study of fluctuating potentials in Cu_2ZnSnS_4 based thin films," *Phys. Rev. B* **84**(2), 024120 (2011), http://dx.doi.org/10.1103/PhysRevB.84.024120.
8. S. Levcenco et al., "Free-to-bound recombination in near stoichiometric Cu_2ZnSnS_4 single crystals," *Phys. Rev. B* **86**(4), 045206 (2012), http://dx.doi.org/10.1103/PhysRevB.86.045206.
9. M. Grossberg et al., "Photoluminescence and Raman study of $Cu_2ZnSn(Se_xS_{1-x})_4$ monograins for photovoltaic applications," *Thin Solid Films* **519**(21), 7403–7406 (2011), http://dx.doi.org/10.1016/j.tsf.2010.12.099.
10. H. Yoo, J. Kim, and L. Zhang, "Sulfurization temperature effects on the growth of Cu_2ZnSnS_4 thin film," *Current Appl. Phys.* **12**(4), 1052–1057 (2012), http://dx.doi.org/10.1016/j.cap.2012.01.006.
11. M. Grossberg et al., "The role of structural properties on deep defect states in Cu_2ZnSnS_4 studied by photoluminescence spectroscopy," *Appl. Phys. Lett.* **101**(10), 102102 (2012), http://dx.doi.org/10.1063/1.4750249.
12. A. P. Levanyuk and V. V. Osipov, "Edge luminescence of direct-gap semiconductors," *Sov. Phys. Usp.* **24**(3), 187–215 (1981), http://dx.doi.org/10.1070/PU1981v024n03ABEH004770.
13. B. I. Shklovskii and A. L. Efros, *Electronic Properties of Doped Semiconductors*, Springer, *Heidelberg, Berlin and New York* (1984).
14. J. Krustok et al., "The role of spatial potential fluctuations in the shape of the PL bands of multinary semiconductor compounds," *Physica Scripta* **T79**, 179–182 (1999), http://dx.doi.org/10.1238/Physica.Topical.079a00179.

15. A. Jagomägi et al., "Photoluminescence studies of heavily doped $CuInTe_2$ crystals," *Physica B* **337**(1), 369–374 (2003), http://dx.doi.org/10.1016/S0921-4526(03)00429-0.
16. J. Krustok et al., "Photoluminescence properties of polycrystalline $AgGaTe_2$," *Solar Energy Mater. Solar Cells* **90**(13), 1973–1982 (2006), http://dx.doi.org/10.1016/j.solmat.2006.02.003.
17. J. Krustok et al., "On the shape of the close-to-band-edge photoluminescent emission spectrum in compensated $CuGaSe_2$," *phys. stat. sol. (a)* **173**(2), 483–490 (1999), http://dx.doi.org/10.1002/(ISSN)1521-396X.
18. M. J. Romero et al., "Comparative study of the luminescence and intrinsic point defects in the kesterite Cu_2ZnSnS_4 and chalcopyrite $Cu(In, Ga)Se_2$ thin films used in photovoltaic applications," *Phys. Rev. B* **84**(16), 165324 (2011), http://dx.doi.org/10.1103/PhysRevB.84.165324.
19. P. K. Sarswat and M. L. Free, "A study of energy band gap versus temperature for Cu_2ZnSnS_4 thin films," *Physica B* **407**(1), 108–111 (2012), http://dx.doi.org/10.1016/j.physb.2011.09.134.
20. S. Chen et al., "Crystal and electronic band structure of Cu_2ZnSnX_4 (X = S and Se) photovoltaic absorbers: first-principles insights," *Appl. Phys. Lett.* **94**(4), 041903 (2009), http://dx.doi.org/10.1063/1.3074499.
21. T. Schmidt, K. Lischka, and W. Zulehner, "Excitation-power dependence of the near-band-edge photoluminescence of semiconductors," *Phys. Rev. B* **45**(16), 8989–8994 (1992), http://dx.doi.org/10.1103/PhysRevB.45.8989.